



Clinical research

Detection of coronary artery disease by magnetic resonance myocardial perfusion imaging with various contrast medium doses: first european multi-centre experience

T.H. Giang^a, D. Nanz^b, R. Coulden^c, M. Friedrich^d, M. Graves^c, N. Al-Saadi^d, T.F. Lüscher^a, G.K. von Schulthess^b, J. Schwitter^{a,*}

^a Division of Cardiology, University Hospital Zurich, Raemistrasse 100, CH-8091 Zurich, Switzerland

^b Department of Medical Radiology, University Hospital Zurich, Raemistrasse 100, CH-8091 Zurich, Switzerland

^c University Hospital Cambridge

^d Franz Volhard Klinik, Berlin

Received 10 February 2004; revised 16 June 2004; accepted 24 June 2004

Available online 21 August 2004

KEYWORDS

Magnetic resonance imaging;
Perfusion;
Coronary disease

Aims Magnetic resonance (MR) first-pass myocardial perfusion imaging during hyperaemia detects coronary artery stenoses in humans with test sensitivity depending on contrast medium (CM)-induced signal change in myocardium. In this prospective multi-centre study, the effect of CM dose on myocardial signal change and on diagnostic performance was evaluated using a stress-only approach.

Methods and results Ninety-four patients with known or suspected coronary artery disease (CAD) were randomised to 0.05, 0.10, or 0.15 mmol/kg body weight of an extravascular CM (Gd-DTPA) and X-ray coronary angiography was performed within 30 days prior/after the MR examination. A multi-slice MR technique with identical hardware and software in all centres was used during hyperaemia (adenosine 0.14 mg/kg/min) to monitor myocardial CM wash-in kinetics and data were analysed semi-automatically in a core laboratory. Protocol violations resulted in 80 complete studies with CAD (defined as ≥ 1 vessel with diameter stenosis $\geq 50\%$ on quantitative coronary angiography) present in 19/29, 13/24, and 20/27 patients for doses 1, 2, and 3, respectively. In normal myocardium, the upslope increased with CM dose (overall- $p < 0.0001$, ANOVA). For CAD detection the area under the receiver operator characteristics curve for subendocardial data (3 slices with quality score < 4 representing 86% of cases) was 0.91 ± 0.07 and 0.86 ± 0.08 for doses 2 and 3, respectively, and was lower for dose 1 (0.53 ± 0.13 , $p < 0.01$ and $p < 0.02$ vs. doses 2 and 3, respectively). Corresponding sensitivities/specificities (95% confidence intervals) for pooled doses 2/3 were 93% (77–99%; ns vs. dose 1) and 75% (48–92%; $p < 0.05$ vs. dose 1), respectively.

* Corresponding author. Tel.: +41 1 255 38 71; fax: +41 1 255 44 01.
E-mail address: juerg.schwitter@dmr.usz.ch (J. Schwitter).

Conclusions With increasing doses of CM, a higher signal response in the myocardium was achieved and consequently this stress-only protocol, with CM doses of 0.10–0.15 mmol/kg combined with a semi-automatic analysis, yielded a high diagnostic performance for the detection of CAD.

© 2004 The European Society of Cardiology. Published by Elsevier Ltd. All rights reserved.

Introduction

In recent years MR perfusion imaging has emerged as an alternative tool to study regional myocardial perfusion, but several conceptual and technical aspects of the imaging protocol remain controversial. In MR perfusion studies, hypoperfused myocardium shows delayed contrast medium (CM) wash-in kinetics during first-pass.^{1–6} Since detection of hypoperfused myocardium is facilitated by augmenting the difference between first-pass signal change in normal vs. hypoperfused myocardium,⁷ i.e., by increasing the dynamic range of signal response in normal myocardium, pulse sequence parameters and dose of CM are important to maximize peak signal in normal myocardium during first-pass. Typically, doses of 0.025 mmol/kg,⁴ 0.03 mmol/kg,⁸ 0.04 mmol/kg,⁹ 0.05 mmol/kg,⁶ and 0.1 mmol/kg^{7,10} were used for first-pass MR perfusion imaging in humans. While high CM doses may increase the dynamic range of myocardial signal response, susceptibility artefacts at higher doses could cause signal loss and result in false positive findings. Patients were therefore randomly assigned to 0.05, 0.10, and 0.15 mmol/kg of an extravascular CM. Here, we were particularly interested to determine the dose with best performance when data were analysed semi-automatically, i.e., with minimal observer interference (i.e., data registration and contour drawing only). As a measure of perfusion, this analysis yielded signal change/time (i.e., the up-slope) which was shown to correlate well with myocardial perfusion.^{1,10} Based on previous reports^{6,10} suggesting that the subendocardial layer is the most sensitive to ischaemia, all analyses were performed in the subendocardial layer and for full wall thickness.

In a recent single centre MR perfusion study¹⁰ hyperaemic data alone allowed for reliable stenosis detection. Such a stress-only approach is advantageous in comparison to rest-stress protocols, since it shortens both time for examination and analysis. Finally, to address the impact of data quality on test performance, data from 3 different MR centres were entered into this study.

Methods

Study population

Ninety-four patients scheduled for coronary angiography were enrolled in 3 centres in order to assess the diagnostic efficacy of 3 doses of an extravascular CM. Coronary angiography was

indicated in the presence of clinical suspicion (based on symptoms and/or positive findings of ischaemia testing with conventional methods) or as part of routine work-up prior to surgery of the great vessels. This resulted in a prevalence of 65% for CAD (defined as $\geq 50\%$ diameter stenosis in any coronary artery) which reflects the typical population undergoing coronary angiography in these centres. Exclusion criteria in this open-label phase II trial were recent myocardial infarction (<2 weeks prior to enrollment), unstable angina, atrial fibrillation, 2nd/3rd degree AV block, and previous coronary artery bypass grafting.

Patients were randomised (balanced for each centre) to either 0.05, 0.10, or 0.15 mmol/kg body weight of Gd-DTPA (Magnevist, Berlex Laboratories, NJ, USA). X-ray coronary angiography was performed within 30 days prior/after the MR study (without any interventions or changes in symptoms between the studies). Antianginal medication was withdrawn ≥ 24 h before the MR study as were caffeinated beverages or food. During the 2 h prior to and immediately after the MR examination, as well as 2–4 and 24 h later, vital signs and 12-lead ECG recordings were performed. Blood samples were collected prior to and 2–4 and 24 h after the MR examination.

The study protocol was approved by the local Ethics Committees and all subjects gave written informed consent prior to study participation. MR and angiographic data were analysed and stored without knowledge of the patients history, symptoms, or findings obtained during the other procedures.

MR examination

All subjects were examined in the supine position using 1.5T MR scanners (CV/i, General Electric, Milwaukee, WI, USA), identical phased-array receiver coils, ECG-triggering devices, and the same pulse sequence software.¹¹ Following 3 min of adenosine infusion (0.14 mg/kg/min), Gd-DTPA was injected into a cubital vein at 5 mL/s (Spectris, Medrad®, Indianapolis, PA, USA), and adenosine was stopped after first-pass data acquisition. Coincident with initiation of imaging and CM injection, the patient held his/her breath to reduce motion artefacts during first-pass. Peak CM effect was achieved at approximately 20 heart beats, while total acquisition lasted 60 heart beats. CM first-pass through the heart was monitored using a hybrid echo-planar pulse sequence (TR 6.6–15.8 ms, TE 1.3–2.2 ms, delay time (=time between 90° preparation pulse and read-out): 158–211 ms, echo-train length 4–8, field-of-view 34–37 × 25–27 cm, matrix 128 × 128, slice thickness 10 mm, and read-out flip angle 25°). Depending on heart rate, 6–8 interleaved short-axis slices were acquired over two full R–R intervals (systole and diastole).¹¹ During the MR study blood pressure and heart rate were acquired at 2, 5, 15, 30, 60 min after CM administration. Two-lead ECG, respiratory rate, and oxygen saturation were monitored continuously (Model 9500, MR Equipment, Bay Shore, NY).

Data analysis

MR data analysis was performed in a core laboratory by an experienced observer blinded to any clinical or invasive data. To correct for gross cardiac motion, several anatomic landmarks (epicardial/endocardial borders, papillary muscles) were aligned manually using a home-written software. Quality of the registered data was assessed by 2 blinded readers by consensus using a 14-point scoring system; 2 points each were assigned to residual motion during CM wash-in, ghosts along phase-encoding, and susceptibility, 1 point was assigned to motion after CM wash-in, blurring along phase-encoding, double contours, extra systoles, and blood pool or coronary arteries included in myocardial drawings. With this rating a score ≥ 4 defined visually non-evaluable studies. Epicardial and endocardial contours were drawn on the registered images (excluding papillary muscles) and eight equiangular segments/slice were generated automatically (rotating clockwise using the anterior septal insertion of the right ventricle as a reference).¹⁰ The maximum upslope (5-point linear fit, sliding window) was calculated for full wall thickness and the inner half, i.e., the subendocardial layer, in 48–64 segments/heart (depending on the number of slices acquired).

In order to evaluate the effect of the 3 CM doses on signal increase in normal myocardium, absolute upslope values in the subendocardial and transmural segments were calculated in the patients without CAD (diameter stenoses < 50% on quantitative coronary angiography; QCA). To correct for surface coil inhomogeneity, relative upslope values were calculated by dividing signal change during first-pass by the pre-contrast signal.

Receiver operator characteristics of MR perfusion imaging vs. X-ray coronary angiography

CAD was defined as ≥ 1 stenosis $\geq 50\%$ in diameter in any of the 3 coronary arteries (and their side branches with a diameter ≥ 2 mm) on QCA (Philips Inturys, R2.2). QCA was performed on-site with the observers blinded to all clinical and MR data (data from the University Hospital Cambridge were analysed in the University Hospital Zurich for logistical reasons).

Since a minimum of 6 slices was acquired in all patients and the first slice had inconsistent preparation (see Fig. 1(c)/(g)/(l)), 5 slices were used for ROC analyses, which were performed on a patient basis (i.e., ≥ 1 segment of a total of 40 segments/heart below threshold was required to define the presence of CAD in a patient on MR). To assess the diagnostic performance of subendocardial and transmural upslope data, ROC curves were generated from 100 sensitivity/specificity pairs per dose by generating 100 thresholds per dose defined as $\text{slope}_{\text{norm}} - x \cdot \text{SD}$ with x increasing in steps of 0.1, and $\text{slope}_{\text{norm}}$ being the normalised slope; since 3 different CM doses were used in this study, upslopes in normal myocardium (=patients without CAD) were expressed as a fraction of the mean upslope value for each dose. Through this normalisation, $\text{slope}_{\text{norm}}$ of the 3 CM dose groups becomes interchangeable, i.e., for the thresholds for dose 1, $\text{slope}_{\text{norm}}$ was calculated as the mean of $\text{slope}_{\text{norm}}$ from the patients without CAD of dose 2 ($n = 11$) and 3 ($n = 7$). Thus, no data of dose 1 were used to generate threshold values for the calculation of ROC curves of dose 1. In analogy, for ROC analysis of dose 2, $\text{slope}_{\text{norm}}$ was calculated as means of $\text{slope}_{\text{norm}}$ from the patients without CAD of dose 1 ($n = 10$) and 3 ($n = 7$). For ROC analysis of dose 3, $\text{slope}_{\text{norm}}$ was calculated as means of $\text{slope}_{\text{norm}}$ from the patients without CAD of dose 1 ($n = 10$) and 2 ($n = 11$). Finally, $\text{slope}_{\text{norm,endo}} \pm \text{SD}$ and $\text{slope}_{\text{norm,trans}} \pm \text{SD}$ refer to mean slopes $\pm \text{SD}$ derived from the subendocardial layer and from full wall thickness, respectively.

All ROC analyses were performed for subendocardial and transmural upslopes of 5 slices (=entire stack) and of the central 3 slices. Calculations were repeated after eliminating studies with lowest image quality (=quality score ≥ 4). These data were also analysed by a second observer to determine reproducibility.

Diagnostic performance of MR perfusion imaging was also assessed in single and multi-vessel disease and for various coronary arteries (with segments 1 and 8 assigned to the left anterior descending coronary artery, segment 3 to the left circumflex, and segments 5 and 6 to the right coronary artery and their corresponding branches¹⁰).

Statistical analysis

Values are given as mean \pm SD. To compare absolute and relative signal changes as well as upslope data in the various segments and slices for the 3 CM doses an ANOVA for repeated measurements was performed (within factors: segments or slices, between factor: CM dose) followed by Scheffe's post hoc testing. Sensitivities and specificities including 95% confidence intervals were calculated on a patient basis with an exact binomial test. Comparisons between doses for sensitivities and specificities were performed by Fisher's exact test. ROC curves were generated as described above on a patient basis and were compared according to Hanley et al.,^{12,13} followed by Bonferroni-correction to address the problem of multiple comparisons ($p < 0.017$ = significant). All tests were 2-sided and a $p < 0.05$ was considered statistically significant.

Measuring an expected difference in upslope between dose groups of approximately $10\%/s$ ¹¹ with an inter-observer reproducibility of approximately $10\%/s$ ¹⁰ in 3 groups with 30 patients each was calculated to yield an estimated power of 91% to detect differences at a p -value of 0.017 (=0.05/3).

Results

In 14 patients out of 94, data were incomplete due to incorrect study protocol in 10 (6 uncorrected MR pulse sequences, 4 missing coronary angiography), 2 images lost before archiving, paravenous CM administration and 1 claustrophobia. No serious adverse events were reported. Demographics and haemodynamics are given in Table 1. No patients with persistent left bundle branch block were studied.

Myocardial signal response in normal myocardium

Fig. 1 shows the signal intensity–time curves in normal myocardium (patients without CAD on QCA) for all 3 CM doses. Fig. 1(a)/(e)/(i) demonstrates the typical effect of inhomogeneous coil sensitivity causing reduced signal reception from segments distant from the coil (segments 4–6). An efficient correction for signal differences between segments is achieved by division of the first-pass signal intensity by the pre-contrast signal intensity (Fig. 1(b)/(f)/(k)). This procedure also corrects for different distances of the various myocardial slices from the receiver coil (Fig. 1(c)/(g)/(l)). However, this approach does not fully account for different signal

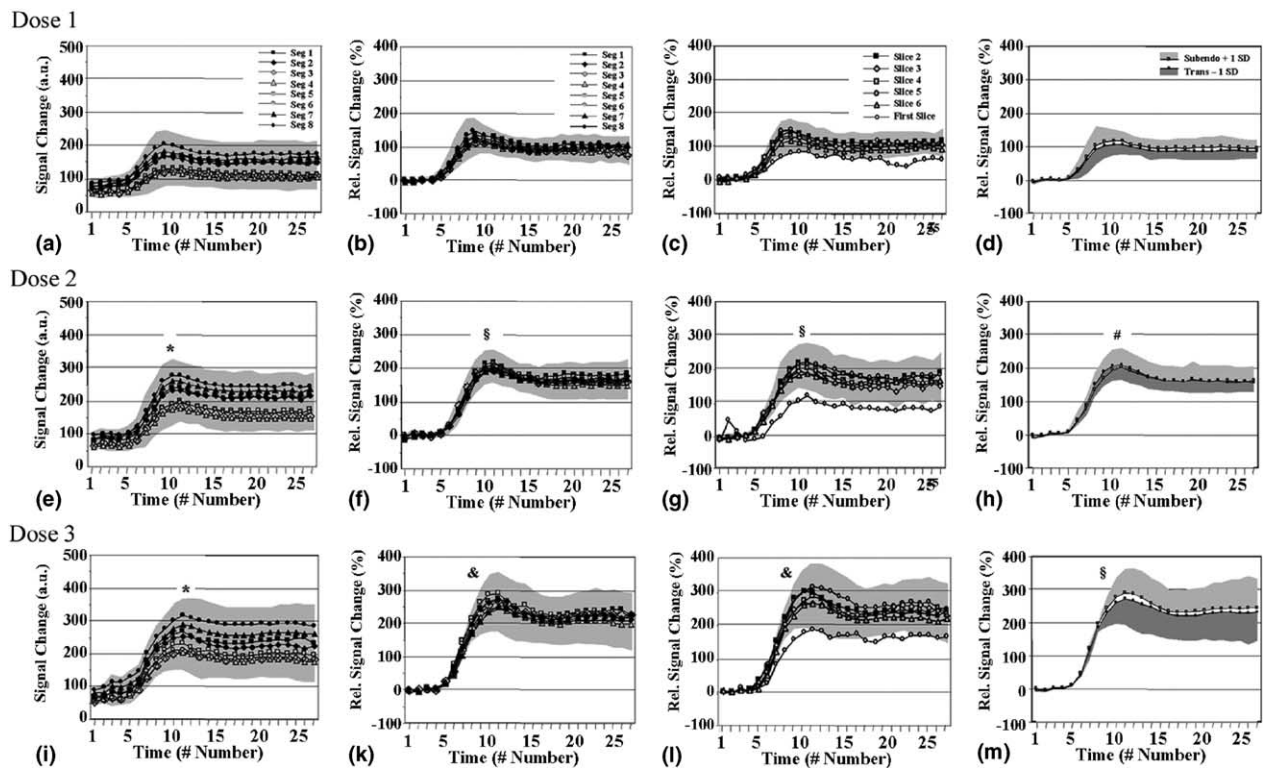


Fig. 1 Signal intensity-time curves in normal myocardium for all 3 contrast medium doses are shown. Absolute signal change (peak signal – pre-contrast signal) in anterior and antero-septal segments (1, 2 and 7, 8, respectively) located closely to the surface coil is high in comparison with the more distant segments 3–6 (a/e/i). Relative signal change (b/f/k) corrects for response differences in the various segments. Relative signal change also corrects for response differences between slices 2–6, but not for slice 1 ($p < 0.0001$ vs. all other slices; c/g/l). Finally, Figure 1d/h/m demonstrates that no susceptibility-induced signal loss occurs in the subendocardium even at the highest dose of 0.15 mmol/kg of Gd-DTPA. The grey areas represent ± 1 SD of the curves of all patients (without coronary stenoses) for segments 1–8 (all slices/heart averaged, panels a/b/e/f/i/k), for slices 2–6 (all segments/heart averaged, c/g/l), and for subendocardial and full thickness data (all segments/heart averaged, d/h/m). * $p < 0.02$ vs. dose 1, $^{\#}p < 0.0001$ vs. dose 1, $^{\&}p < 0.05$ vs. dose 1 (repeated measures ANOVA with Scheffe post hoc testing). Significance levels in (h) and (m) apply for both, subendocardial and full wall thickness data.

properties in slice 1, acquired first after the R wave, where the magnetisation preparation differs from that of the other slices. Finally, Fig. 1(d)/(h)/(m) demonstrates that signal increase in the subendocardial layer is not different from full wall thickness data for all doses. Even at the highest dose of 0.15 mmol/kg (Fig. 1(m)), no susceptibility-induced signal loss, but a further increase in signal in the subendocardium is noted ($p < 0.02$ vs. 0.10 mmol/kg, ANOVA with Scheffes post hoc testing). As shown for signal change, upslope values (%signal change/s) also increased with increasing CM doses. For doses 1, 2, and 3 in the subendocardium: $24.9 \pm 9.0\%/s$, $37.0 \pm 6.3\%/s$ ($p < 0.02$ vs. dose 3; $p = 0.6$ vs. dose 1), and $47.4 \pm 14.9\%/s$ ($p < 0.0001$ vs. dose 1), respectively.

Diagnostic performance of MR perfusion imaging

For the dose groups 1–3, mean quality scores were similar (1.9 ± 1.6 ; 2.2 ± 1.6 ; and 1.6 ± 1.4 , respectively, not significant). A total of 11 studies (14%, 17%, and 11% for dose groups 1–3, respectively) were deemed non-evaluable by visual assessment (score ≥ 4 ; 14% of all studies, no

significant differences for the 3 centres). ROC analyses were performed on both, patients with adequate quality ($n = 69$; score < 4) and on the entire data set.

Best diagnostic performance was achieved for doses 2 and 3 in studies with adequate quality (score < 4) when analysis was restricted to the 3 central slices (subendocardial data, Fig. 2(a)). Sensitivity and specificity (absolute numbers and 95% confidence intervals in parenthesis) for dose 2 were 91% (10/11; 59–100%) and 78% (7/9; 40–97%), respectively, and for dose 3, 94% (16/17; 71–100%) and 71% (5/7; 29–96%), respectively. For dose 1, at a comparable sensitivity level of 94% (16/17; 71–100%, ns vs. doses 2 and 3), specificity was only 25% (2/8; 3–65%, $p = 0.057$ vs. dose 2, $p = 0.13$ vs. dose 3). For the pooled doses 2 and 3 (subendocardial data), sensitivity and specificity were 93% (26/28; 77–99%, ns vs. dose 1) and 75% (12/16; 48–92%, $p > 0.05$ vs. dose 1), respectively. Negative/positive predictive values for doses 1, 2, and 3 were 73/67%, 88/83% and 83/89%, respectively.

With respect to data quality, most artefacts were motion-related (82% of all images with a score ≥ 4). Cardiac coverage may affect data quality by increasing partial volume artefacts in apical slices or by including atria

Table 1 Patient demographics

	Dose 1 (0.05 mmol/kg)	Dose 2 (0.10 mmol/kg)	Dose 3 (0.15 mmol/kg)
Total: <i>n</i>	29	24	27
Age (years)	58 ± 8	57 ± 9	58 ± 10
Gender (male/female)	25/4	16/8	24/3
Body weight (kg)	80 ± 11	76 ± 11	81 ± 15
Risk factors			
hypertension	13 (45)	7 (29)	11 (41)
Hypercholesterolemia	17 (59)	11 (46)	17 (63)
Smoking	10 (34)	8 (33)	10 (37)
Diabetes mellitus	4 (14)	3 (13)	5 (19)
Family history	5 (17)	4 (17)	4 (15)
Prior myocardial infarctions	11 (38)	7 (29)	10 (37)
History of heart failure	0 (0)	3 (13)	1 (4)
Atypical or no chest pain	2 (7)	2 (8)	2 (7)
Angina pectoris			
CCS I	14 (48)	10 (42)	10 (37)
CCS II	8 (28)	11 (46)	9 (33)
CCS III	5 (17)	3 (13)	4 (15)
CAD			
1-CAD	10 (34)	9 (38)	11 (41)
2-CAD	8 (28)	2 (8)	3 (11)
3-CAD	1 (3)	2 (8)	6 (22)
Prior PCI	3 (10)	6 (25)	8 (30)
Time to MR in months: range [mean]	6–7 [6.3]	3–65 [24.7] ^a	3–7 [5.7]
Correct diagnosis by MR	1	6	6
Therapy ^b			
Conservative therapy only	12 (41)	10 (42)	15 (56)
PCI	10 (34)	9 (38)	8 (30)
CABG	5 (17)	4 (17)	4 (15)
Resting condition			
Heart rate (bpm)	67 ± 10	68 ± 11	67 ± 9
Systolic BP (mmHg)	145 ± 21	142 ± 21	149 ± 22
Diastolic BP (mmHg)	81 ± 10	80 ± 12	81 ± 12
Stress condition ^c			
heart rate (bpm)	72 ± 13	75 ± 15	75 ± 13
systolic BP (mmHg)	142 ± 23	143 ± 24	146 ± 28
diastolic BP (mmHg)	78 ± 11	77 ± 12	80 ± 12

Numbers in parentheses represent percentages. No statistically significant differences between dose groups were present.

^a In one patient a percutaneous coronary intervention (PCI) was performed 2 days prior to MR which yielded correct results.

^b Therapy following coronary angiography and MR examination.

^c At 2 min after end of adenosine infusion. bpm, beats/min; BP, blood pressure; CABG, coronary artery bypass grafting; 1-, 2-, 3-CAD, single-, double-, tripple-vessel coronary artery disease; CCS, Canadian Cardiovascular Society. All patients were taking acetyl salicylic acid and statins if indicated.

and/or the membranous portion of the interventricular septum in basal slices. When control of artefacts was less strict by either analysing the entire stack of slices (Fig. 2(c)) or by including images of all quality scores (Fig. 2(b)), performance of dose 2 tended to deteriorate (ns vs. dose 2 in Fig. 2(a)). When control of artefacts was lowest (analysis of entire stack of slices for all quality scores, Fig. 2(d)) AUC for dose 2 decreased further ($p < 0.05$ vs. dose 2 with 3 slices and score < 4 , Fig. 2(a)). Dose 1 performed poor under all circumstances. Dose 3 appeared most robust with high AUCs for any type

of sub-analysis. Despite similar distribution of 1-, 2-, and 3-vessel disease (VD) in all 3 dose groups (see Table, statistics not significant), sensitivities/specificities were also calculated with 3-VD patients excluded yielding 91/71% for dose 3 (94/71% with 3-VD), 89/78% for dose 2 (91/78% with 3-VD), and 94/25% for dose 1 (94/25% with 3-VD).

Fig. 3 demonstrates a comparable diagnostic performance of the MR perfusion technique in the various myocardial perfusion territories (irrespective of receiver coil distance). Fig. 4 shows the influence of the number

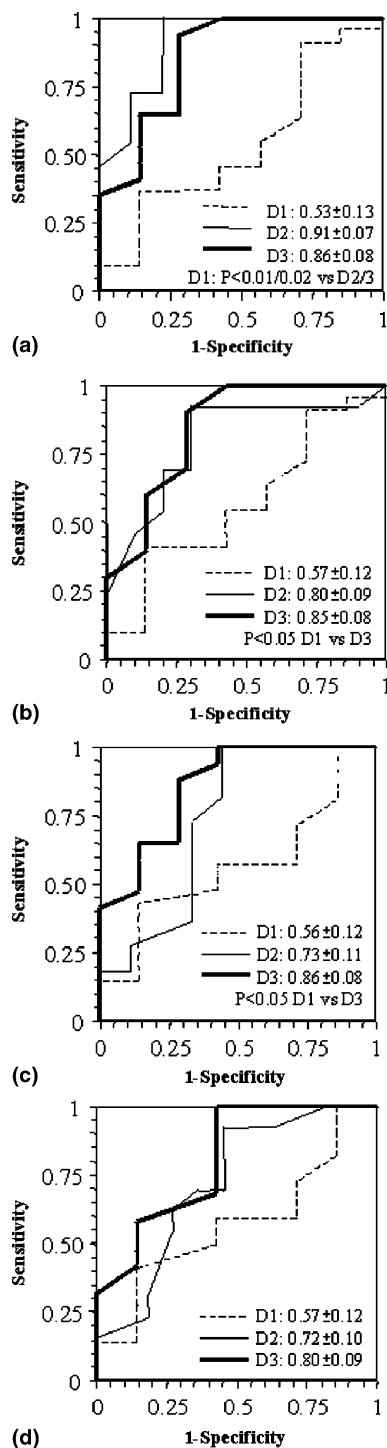


Fig. 2 Receiver operator characteristics (ROC) curves of MR upslope data are shown for the detection of coronary artery disease ($\geq 50\%$ diameter stenosis in ≥ 1 vessel by quantitative coronary angiography). MR upslope data from the subendocardial layer are highly reliable in the detection of disease when analysis is restricted to the central 3 slices in patients with adequate image quality (a). Numbers within the plots represent area under the ROC curve \pm standard error for doses 1, 2 and 3 (=D1, D2, D3, respectively). In less restrictive data sets (analysis of all quality scores, b; and analysis of 5 slices, c), diagnostic performance tended to decrease for doses 2 and 3. AUC of dose 2 for least restrictive data (all slices, all quality scores, d) was worst ($p < 0.05$ vs. dose 2 in a). A dose of 0.05 mmol/kg (=D1) performed inadequately in all analyses. Due to comparisons between 3 doses a $p < 0.017$ is considered significant.

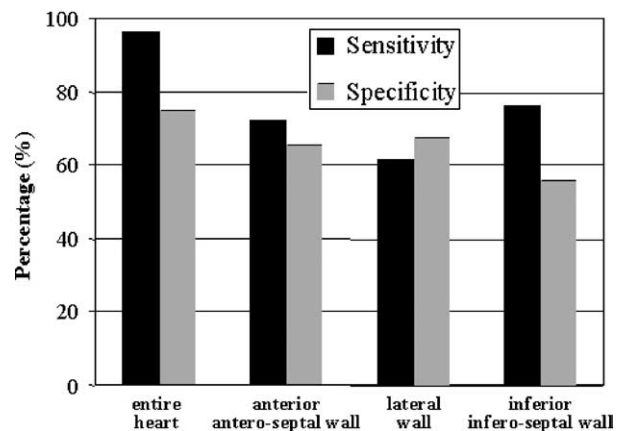


Fig. 3 Diagnostic performance (=sensitivity/specificity of MR perfusion imaging of pooled doses 2 and 3 to detect $\geq 50\%$ diameter stenoses in the various coronary arteries by QCA; 44 patients) was similar in the various perfusion territories and confirms comparable image quality throughout the left ventricular myocardium. In the anterior and antero-septal wall (assigned to the left anterior descending coronary artery) 10 segments were analysed, in the lateral wall (assigned to the left circumflex coronary artery) 5, and in the inferior and infero-septal wall (assigned to the right coronary artery) 10 segments were analysed. For the patient-based analysis (entire heart) all 40 segments per heart were included in the analysis, which increased sensitivity/specificity.

of coronary artery involvement on sensitivity and specificity of MR data. An example is given in Fig. 5.

For all analyses, transmural data performed slightly worse than subendocardial data. However, sample size was too small to achieve statistical significance even after pooling of doses 2 and 3 (AUC of subendocardial and transmural data: 0.88 ± 0.05 and 0.80 ± 0.05 , respectively, not significant). For image registration, contour drawings, and upslope calculations approximately 10, 5, and 1 min were needed, respectively.

For dose group 1, analysis by both observers yielded identical sensitivity and specificity. For dose 2, one patient was missed (=diagnosed as normal) by the analysis of the second observer (compared with the first observer), whereas no difference was found for the controls (sensitivity/specificity: 82/78%, subendocardial data, second observer). Finally, for dose 3, one patient missed by the first observer was detected by the second observer and no difference was found for the controls (sensitivity/specificity: 100/71% for second observer). Mean difference \pm SD for subendocardial upslopes (in 3 central slices of 69 patients) determined by observer 1 and 2 for doses 1, 2, and 3 were: -2.1 ± 3.7 , 0.1 ± 5.6 , and $-0.4 \pm 6.7\%/s$, respectively (for 600, 480, and 576 segments, respectively).

Discussion

This study demonstrates (1) that peak signal response in normal myocardium increases with doses up to 0.15 mmol/kg of an extravascular CM, and (2) a single hyperaemic examination using doses of 0.10 – 0.15 mmol/kg and a signal upslope quantification in the sub-

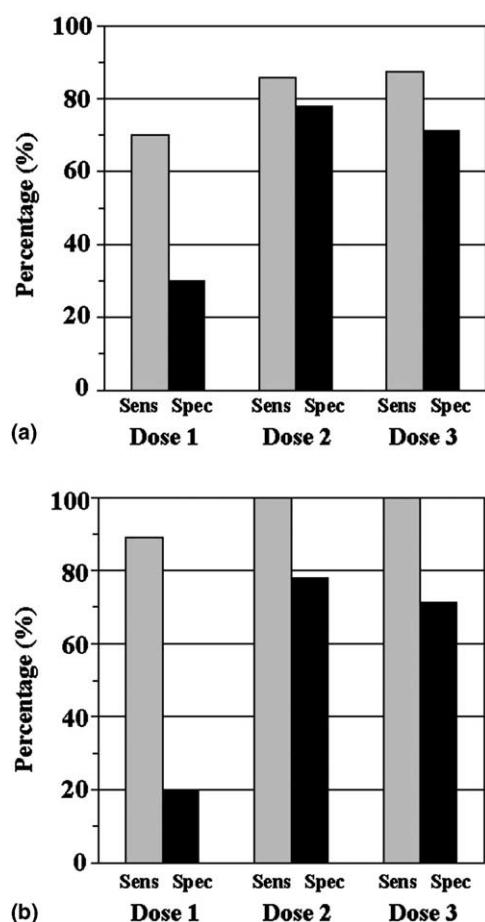


Fig. 4 Sensitivities and specificities for the detection of single-vessel (a) and multi-vessel disease (b) are shown for the 3 contrast medium doses. Sensitivities and specificities were particularly high for doses 2 and 3 in multi-vessel disease (not significant vs. single-vessel disease). At a high sensitivity level, specificity of dose 1 was low ($p = 0.07$ and $p = 0.05$ vs. pooled doses 2 and 3 (data not shown) in single and multi-vessel disease, respectively, Fisher's exact test).

endocardium is a highly reliable method for the detection of CAD.

Diagnostic performance of MR perfusion imaging

The presented MR perfusion technique yields sensitivities/specificities for the detection of CAD of 91/78% (AUC 0.91), and 94/71% (AUC 0.86) for the 2 highest doses of 0.10 and 0.15 mmol/kg of an extravascular CM, respectively. These high sensitivities/specificities are obtained from a single hyperaemic study and are in-line with results of an earlier report¹⁰ with a sensitivity/specificity of 88/86% using a single injection of 0.1 mmol/kg Gd-DTPA-BMA during hyperaemia. A substantial body of evidence from the positron emission tomography (PET) literature supports these findings demonstrating high correlations between percent area stenosis of epicardial coronary vessels and maximal hyperaemic blood flow.^{14,15} Although an MR perfusion reserve approach yielded high sensitivity/specificity as well,⁴ the assessment of hyperaemic perfusion alone confers several

advantages such as a reduced examination time (avoiding a second CM injection and the waiting time between injections), a reduced analysis time (no analysis of resting study), and eliminating the necessity to spatially match the hyperaemic and resting study for the reserve calculation, which might be particularly problematic if analysis is performed for the subendocardium. In addition, myocardial signal response induced by the second CM injection is influenced by the amount of CM still present in the myocardium following the first injection, unless complete wash-out is allowed, which however, would prolong the examination. Finally, hyperaemic perfusion during vasodilation is decoupled from oxygen demand, while perfusion reserve also depends on resting haemodynamics,¹⁶ which may confound the flow-limiting effect of epicardial coronary stenoses.

One prerequisite for a reliable analysis of CM wash-in kinetics is an efficient data correction for inhomogeneous receiver coil sensitivity, which is achieved by division of first-pass data by pre-contrast data (Fig. 1). As a result, sensitivities and specificities for CAD detection are preserved even in territories distant from the surface coil. This might be one major reason for the high overall sensitivities and specificities for detection of CAD of 91–94% and 71–78% for doses 2 and 3, respectively, and even higher sensitivities and specificities were achieved for multi-vessel disease. For comparison, multi-centre single-photon emission computed tomography trials yielded adequate sensitivities of 77–85% but compromised specificities of 50–58%.^{17–19} To our knowledge, only one multi-centre MR perfusion trial has been performed in the past, which achieved a relatively low sensitivity of 57% with a specificity of 85% (using 75% diameter stenosis on QCA as a reference).⁹ These results obtained with 0.04 mmol/kg of a Gd-chelate are in line with the current results of dose 1. The study population consisting of women with a low prevalence of CAD may have further contributed to the rather low test sensitivity in that study.

Contrast medium dose and data quality

Despite the involvement of 3 centres with considerable experience in MR perfusion imaging, data quality was heterogeneous which led us to apply a scoring system for quality. Over 80% of artefacts during CM first-pass were breathing-related and/or degraded by ECG mistriggering. Another source of image degradation is related to cardiac coverage. In more apical slices, partial volume artefacts are more relevant, whereas in the most basal slices, the left atrium and/or the membranous portion of the interventricular septum may be included, where CM wash-in kinetics of myocardium do not apply. In this study triggering was set to every second R-wave and interleaved acquisitions occurred during all cardiac phases clearly affecting the quality of the slices acquired during rapid cardiac motion, i.e., in early-mid systole and early diastole. Accordingly, best quality was present in the central 3 slices (minor partial volume artefacts, no acquisition during rapid cardiac motion) of studies with a quality score < 4

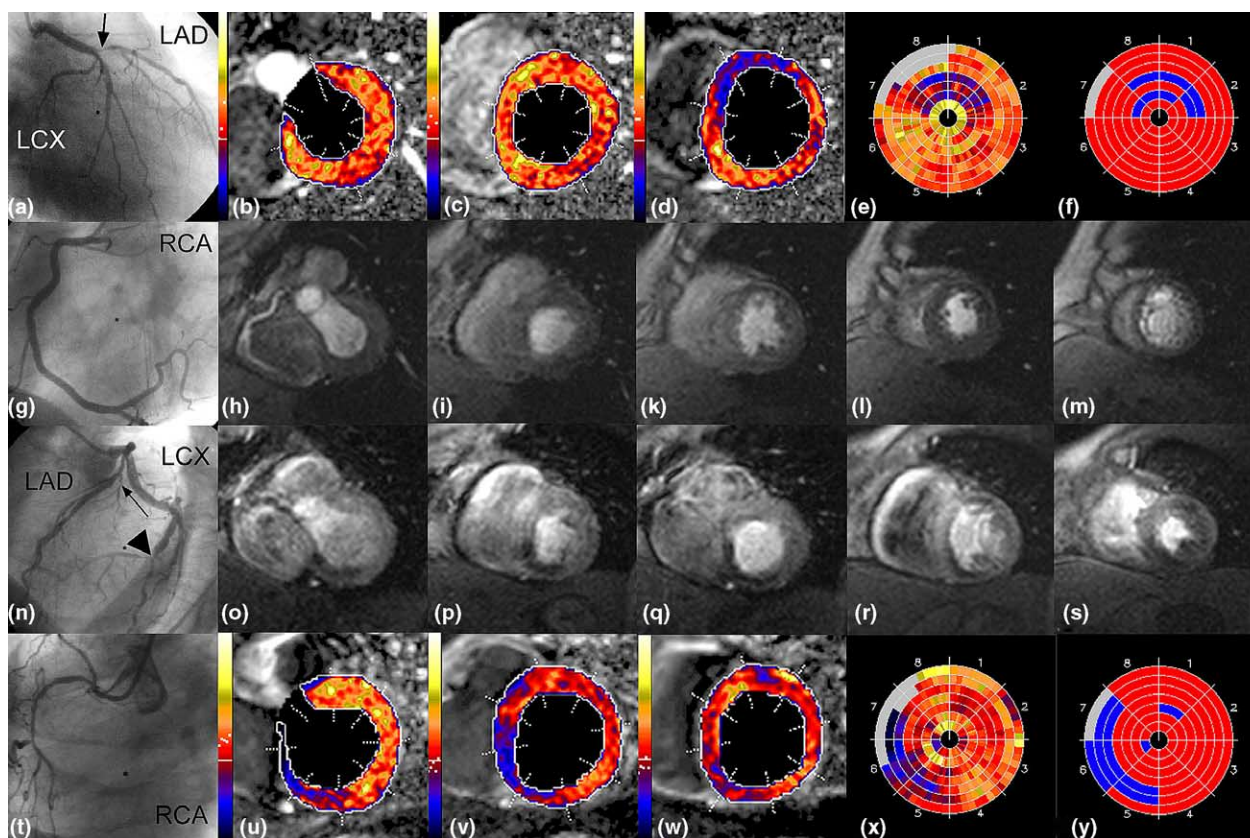


Fig. 5 Examples of MR perfusion studies for dose 1 (top rows a–m) and dose 3 (bottom rows n–y). For dose 1, a stenosis in the left anterior descending coronary artery (LAD) is shown on X-ray angiography (arrow in a) with 5 short-axis MR perfusion images at peak bolus effect in h–m demonstrating low signal areas in the anterior wall (k–l). Corresponding upslope maps are shown in b–d and polar maps for the subendocardial layer are given with thresholds applied pixel-wise (e) and for entire segments (f) with blue/red encoding for upslope values below/above the thresholds, respectively (the polar maps show all acquired slices, for ROC analyses only the central 5 slices were used, for reasons see text). For dose 3, stenoses in the small first diagonal branch of the LAD (arrow in n) and the large left circumflex coronary artery (LCX) are shown (arrowhead in n). For dose 1, note the considerable noise and reduced dynamic range of signal response (h–m) compared with dose 3 (o–s). Upslope maps and subendocardial polar maps for dose 3 (u–y) are generated as explained for dose 1. The second patient (dose 3) further demonstrates the limitation of using coronary anatomy as a reference for perfusion studies: perfusion defects in segment 5 and 6 represent a mismatch with the right coronary artery territory in this patient with a stenosis in the large LCX.

(predominantly eliminating breathing artefacts). In these data with best artefact control, doses 2 and 3 showed superiority over dose 1. This finding demonstrates the importance of an adequate CM dose to achieve high upslope values in normally perfused myocardium and thus, to allow its differentiation from delayed wash-in kinetics in stenosis-dependent myocardium when using semi-automatic analysis.

As in earlier studies,^{8,10} a trend towards better diagnostic performance of subendocardial data in comparison with transmural data was found, which indicates that potential susceptibility artefacts at the blood pool–myocardium interface, even at 0.15 mmol/kg, are small and do not compromise the diagnostic performance of semi-automatic upslope calculations.

Limitations

While perfusion assessment by PET and MR showed a high agreement,¹⁰ the PET technique is not widely available. Therefore, stenosis anatomy, as assessed by QCA, was

chosen as the comparator in this multi-centre setting, even though a perfect agreement between perfusion imaging and QCA cannot be expected and is likely to result in an underestimation of the diagnostic yield of perfusion imaging. In particular, assignment of MR perfusion deficits to individual coronary stenoses (as shown in Fig. 3) may be problematic when performed in a systematic and blinded fashion as in this study (which did not consider the extent of perfusion territories of individual vessels nor collaterals).

While sample size allowed to demonstrate inferiority of dose 1 vs. doses 2 and 3 for detection of CAD, the study population was too small to detect differences between subendocardial and transmural data, or to assess the influence of operators on image quality and test performance. Also, women were underrepresented in this study (<20%) and test performance cannot be applied directly to women. The same caveat applies for patients after percutaneous coronary interventions and for those with complete left bundle branch block. Results of the current trial, particularly on how many slices should be analysed, should not be extrapolated for different pulse

sequences or different hardware. Fourteen patients had to be excluded due to partially missing data. As a consequence, we cannot assess whether exclusions were disproportionate in the 3 dose groups with respect to diagnosis, data quality or other aspects, and any bias cannot be excluded with certainty.

In patients with known or suspected CAD, detection of hypoperfused myocardium is important but additional information as to whether hypoperfusion is related to scar tissue or not is essential for an optimal patient management. Accordingly, a viability assessment by delayed enhancement^{20,21} should be added to a perfusion study to allow for a comprehensive diagnostic work-up.

Conclusions

This study demonstrates a high diagnostic performance of MR perfusion imaging for the detection of anatomically defined coronary artery stenoses when performing a semi-automatic analysis of CM wash-in kinetics into the subendocardium in combination with CM doses of 0.10–0.15 mmol/kg. The short examination time of this stress-only MR protocol and the semi-automatic analysis are major advantages of the proposed technique. These multi-centre results also illustrate the importance of data quality which was inadequate in 14% of studies. Larger multi-centre trials are needed to further refine and disseminate the technique.

Acknowledgements

This work was supported by General Electric Medical Systems and Berlex Laboratories.

References

1. Wilke N, Simm C, Zhang J et al. Contrast-enhanced first-pass myocardial perfusion imaging: correlation between myocardial blood flow in dogs at rest and during hyperemia. *Magn Reson Med* 1993;29:485–97.
2. Saeed M, Wendland MF, Sakuma H et al. Coronary artery stenosis: detection with contrast-enhanced MR imaging in dogs. *Radiology* 1995;196:79–84.
3. Schwitter J, Saeed M, Wendland MF et al. Assessment of myocardial function and perfusion in a canine model of non-occlusive coronary artery stenosis using fast magnetic resonance imaging. *J Magn Reson Imaging* 1998;9:101–10.
4. Al-Saadi N, Nagel E, Gross M et al. Noninvasive detection of myocardial ischemia from perfusion reserve based on cardiovascular magnetic resonance. *Circulation* 2000;101:1379–83.
5. Klocke FJ, Simonetti OP, Judd RM et al. Limits of detection of regional differences in vasodilated flow in viable myocardium by first-pass magnetic resonance perfusion imaging. *Circulation* 2001;104:2412–6.
6. Panting JR, Gatehouse PD, Yang GZ et al. Abnormal subendocardial perfusion in cardiac syndrome X detected by cardiovascular magnetic resonance imaging. *N Engl J Med* 2002;346:1948–53.
7. Bertschinger KM, Nanz D, Buechi M et al. Magnetic resonance myocardial first-pass perfusion imaging: parameter optimization for signal response and cardiac coverage. *J Magn Reson Imaging* 2001;14:556–62.
8. Keijzer J, van Rossum A, Wilke N et al. Magnetic resonance imaging of myocardial perfusion in single-vessel coronary artery disease: implications for transmural assessment of myocardial perfusion. *J Cardiovasc Magn Reson* 2000;2:189–200.
9. Doyle M, Fuisz A, Korthright E et al. The impact of myocardial flow reserve on the detection of coronary artery disease by perfusion imaging methods: an NHLBI WISE study. *J Cardiovasc Magn Reson* 2003;5:475–85.
10. Schwitter J, Nanz D, Kneifel S et al. Assessment of myocardial perfusion in coronary artery disease by magnetic resonance: a comparison with positron emission tomography and coronary angiography. *Circulation* 2001;103:2230–5.
11. Slavin GS, Wolff SD, Gupta SN et al. First-pass myocardial perfusion MR imaging with interleaved notched saturation: feasibility study. *Radiology* 2001;219:258–63.
12. Hanley JA, McNeil BJ. The meaning and use of the area under the receiver operating characteristics (ROC) curve. *Radiology* 1982;143:29–36.
13. Hanley JA, McNeil BJ. A method of comparing the areas under receiver operating characteristics curves derived from the same cases. *Radiology* 1983;148:839–43.
14. Uren NG, Melin JA, De Bruyne B et al. Relation between myocardial blood flow and the severity of coronary artery stenosis. *N Engl J Med* 1994;330:1782–8.
15. Di Carli M, Czernin J, Hoh CK et al. Relation among stenosis severity, myocardial blood flow, and flow reserve in patients with coronary artery disease. *Circulation* 1995;91:1944–51.
16. Schwitter J, DeMarco T, Kneifel S et al. Magnetic resonance-based assessment of global coronary flow and flow reserve and its relation to left ventricular functional parameters: a comparison with positron emission tomography. *Circulation* 2000;101:2696–702.
17. Zaret BL, Rigo P, Wackers FJ et al. Myocardial perfusion imaging with 99mTc tetrofosmin. Comparison to 201Tl imaging and coronary angiography in a phase III multicenter trial. Tetrofosmin International Trial Study Group. *Circulation* 1995;91:313–9.
18. He ZX, Iskandrian AS, Gupta NC et al. Assessing coronary artery disease with dipyridamole technetium-99m-tetrofosmin SPECT: a multicenter trial. *J Nucl Med* 1997;38:44–8.
19. Hendel RC, Berman DS, Cullom SJ et al. Multicenter clinical trial to evaluate the efficacy of correction for photon attenuation and scatter in SPECT myocardial perfusion imaging. *Circulation* 1999;99:2742–9.
20. Kim RJ, Wu E, Rafael A et al. The use of contrast-enhanced magnetic resonance imaging to identify reversible myocardial dysfunction. *N Engl J Med* 2000;343:1445–53.
21. Knuesel PR, Nanz D, Wyss C et al. Characterization of dysfunctional myocardium by positron emission tomography and magnetic resonance: relation to functional outcome after revascularization. *Circulation* 2003;108:1095–100.